Lithuanian Journal of Physics
Vol. **64**, No. 2, pp. 101–106 (2024)
ISSN 1648-8504 eISSN 2424-3647
DOI: https://doi.org/10.3952/physics.2024.64.2.3

SEMICONDUCTIVE LEAD ZIRCONATE TITANATE THIN FILMS GROWN BY PULSED LASER DEPOSITION

V. Haronin [a], M. Alexe [b], R. Grigalaitis [a], and J. Banys [a]

[a] *Faculty of Physics, Vilnius University, Saulėtekio 9, 10222 Vilnius, Lithuania*
[b] *Department of Physics, University of Warwick, Coventry CV4 7AL, UK*
Email: vadzim.haronin@ff.vu.lt

Received 12 December 2023; revised 15 December 2023; accepted 18 December 2023

Heterostructures consisting of $PbZr_{0.2}Ti_{0.8}O_3$ epitaxial films on a $SrTiO_3$ (100) substrate with a $La_{0.67}Sr_{0.33}MnO_3$ bottom electrode were prepared by pulsed laser deposition. Plane-parallel capacitor structures were investigated by dielectric spectroscopy and piezoelectric measurement. Shift in a piezoelectric loop indicates that a sample has a small imprinted internal field, directed towards the copper top electrode. Temperature-dependent measurements in a range of 300–500 K were performed to obtain information on the frequency-depending response of the metal–ferroelectric–metal (MFM) structure and to analyze the effect of charge injection through the two Schottky-like contacts. The charge injection process greatly increases the conductivity in the low-frequency region.

Keywords: semiconductors, lead zirconate titanate, thin films, pulsed laser deposition

1. Introduction

Ferroelectric materials, due to their notable dielectric constant, piezoelectric and pyroelectric coefficients, have found diverse applications in fields such as high-κ dielectric materials, transducers, actuators and sensors [1, 2]. Among these materials, lead zirconate titanate (PZT) stands out as a well-known ferroelectric material, particularly for its piezoelectric applications [3].

However, producing thick PZT films with electrical characteristics matching those of the bulk material is a challenging endeavour. This challenge primarily arises from the issues like crack formation [4], the volatility of lead and lead oxide [5], substrate clamping [6], residual stresses [7], and other limitations associated with thin film processing [8].

To address these challenges, various deposition techniques have been developed for PZT film fabrication. These techniques include vapour-phase deposition methods like chemical vapour deposition and physical vapour deposition, as well as chemical methods such as chemical solution deposition (CSD) and the sol–gel method [9]. However, with these methods there are challenges to achieve the precise stoichiometry of the mixed oxide phase [9], the problems with the potential for residual impurities [10] and lower piezoelectric coefficients [11, 12].

To overcome those issues, vapour-phase deposition techniques were used. Pulsed laser deposition (PLD) is particularly promising for PZT film fabrication due to its ability to achieve high deposition rates (>100 nm/h), maintain a high crystalline quality, preserve stoichiometry [13], produce films with an excellent surface morphology and facilitate the fabrication of high-quality devices such as plane-parallel capacitors [14].

The choice of a similar lattice constant for the electrode and substrate is crucial for promoting layer-by-layer film growth and obtaining a high-quality epitaxy, as lattice constant matching is a key parameter in this regard. For our PZT composition the lattice constant at deposition temperature is 3.953 Å [15]. In this context, lanthanum strontium manganite (LSMO) was chosen as the bottom electrode (a = 3.876 Å) [16] and was

deposited on a strontium titanate (STO) substrate (a = 3.905 Å) [17].

Despite the well-known properties of PZT material and many researchers working with its frequency dependence, it was investigated poorly. The primary objective of this research is to investigate the dielectric and piezoelectric properties of PZT films. This investigation involves the fabrication of metal–ferroelectric–metal structures. Top contacts are made using copper and gold materials.

2. Experiment

PLD was used to grow epitaxial oxide heterostructures of $La_{0.67}Sr_{0.33}MnO_3$ (LSMO) and $PbZr_{0.2}Ti_{0.8}O_3$ (PZT) on a (100)-oriented $SrTiO_3$ (STO) single-crystal substrate with a 5 mm^2 area. The STO substrate was ultrasonically cleaned in acetone and isopropanol, chemically etched by buffered hydrofluoric solution and annealed at 1100°C for 2 h to obtain a vicinal surface with atomically flat terraces.

The PZT film was deposited under specific conditions to optimize its growth and properties. The deposition parameters for the PZT film were as follows: a deposition temperature of 555°C, an ambient pressure of 0.2 mbar and a total of 10,000 laser pulses. The laser had a constant energy fluence of 1 J/cm^2. After the deposition, the samples underwent an annealing process in the O_2 atmosphere at a pressure of 200 mbar. The annealing was performed when the temperature reached 250°C and lasted for 30 min. The purpose of annealing was to lower the number of oxygen vacancies and minimize film leakage. The samples were then cooled at a rate of 20°C/min. The resulting film had an approximate thickness of 100 nm.

The dielectric properties of the films were measured by an HP4284A LCR meter with a needle probe station to cover a 20 Hz – 1 MHz frequency band in the temperature range between 300 and 500 K. Needles were connected to a top electrode and a holder, with a connection to a bottom contact by painting the rear side of the sample with silver paste. The temperature was measured with a *Keithley* Integra 2700 multimeter connected to the probe station. Ferroelectric properties were then investigated by the *aixACCT* measurements system at room temperature.

Top copper and gold (each 25 nm) contacts were sputtered using a metal mask. Copper was deposited directly on the PZT layers to increase the durability of the top contact pad during needle connections to the device. The contact area was 250 μm^2 to reduce the number of defects inside one device.

3. Results and discussion

Typical hysteresis loops for the polarization and the current of the sample are presented in Fig. 1.

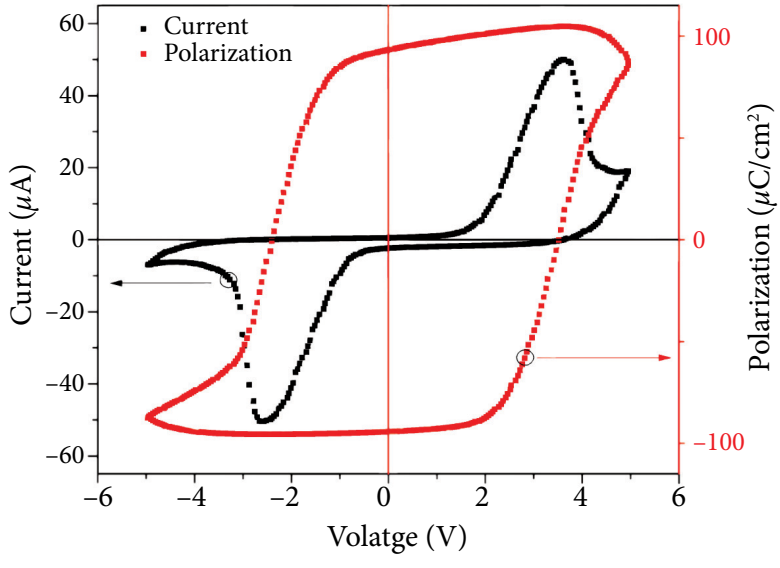

Fig. 1. Polarization and current hysteresis loops obtained for an LSMO/PZT/Cu/Au ferroelectric capacitor by applying a triangular voltage pulse with a frequency of 1 kHz.

The polarization loop exhibits a typical ferroelectric behaviour, with a distinct remnant polarization and coercive voltage. Similarly, the current loop displays hysteresis, indicating the presence of ferroelectric behaviour in the capacitor.

The polarization reversal (ferroelectric switching) within the sample is indicated by the positive and negative notable peaks of the measured current. Remanent polarization is 93 μC/cm^2, which is the usual value for the strained tetragonal 20/80 PZT [18]. Furthermore, it is worth noting that the experimentally obtained polarization value P_r is higher than the theoretical value of 70 μC/cm^2, which is typically calculated for bulk single crystals, as reported in Ref. [19].

The piezoelectric loop has a small shift toward the positive side of the loop that could suggest that there is a small internal field (E_{in}) directed towards the top electrode because of the different types of electrodes that were used. This internal field is commonly linked to defect pairs that comprise negatively charged acceptor ions and positively charged oxygen vacancies, creating electric dipoles [20]. The current–voltage (*IV*) curve shows a significant leakage at high fields limiting the range of applied fields.

The dielectric constant was estimated from the capacitance measurements (see Fig. 2). It has been observed that the dielectric loss, which usually occurs due to the relaxation of space charge and domain walls, reduces as the frequency increases. The observed dispersions in high-frequency tails can be accurately modelled by classical Cole–Cole functions. However, these functions fail to predict the low-frequency plateaus of ε and σ, and instead, a function of the constant phase-angle (CPA) type appears to provide a more accurate description of the data in the low-frequency region of the plots, which could be explained in our case by big numbers of charge carriers, that change the behaviour of our material from a dielectric to a semiconductor [21].

Fit was made with this formula (1), which also considers the contribution of conduction, that may be encountered experimentally at the low-frequency side, proposed by Raicu [22]:

$$\varepsilon(\mathrm{i}\omega) = \varepsilon_\infty + \frac{\sigma}{\mathrm{i}\omega} + \frac{\varepsilon_0 - \varepsilon_\infty}{[(\mathrm{i}\omega\tau)^\alpha + (\mathrm{i}\omega\tau)^{1-\beta}]^\gamma}. \quad (1)$$

Here ε_∞ is the dielectric constant at infinite frequency, ε_0 is the dielectric constant at static field, σ is the conductivity of the film, ω is the measured frequency, τ is the characteristic relaxation time; α, β and γ describe the asymmetry and broadness of the corresponding spectra.

Figure 3 illustrates the relationship between the mean relaxation time and the inverse temperature. The data points represent the fitting results obtained by approximating the frequency dependences of the dielectric permittivity with an account of a low-frequency permittivity, as well as approximating the data using the Arrhenius equations [20]:

$$\tau = \tau_0 \exp\left(\frac{E}{kT}\right). \quad (2)$$

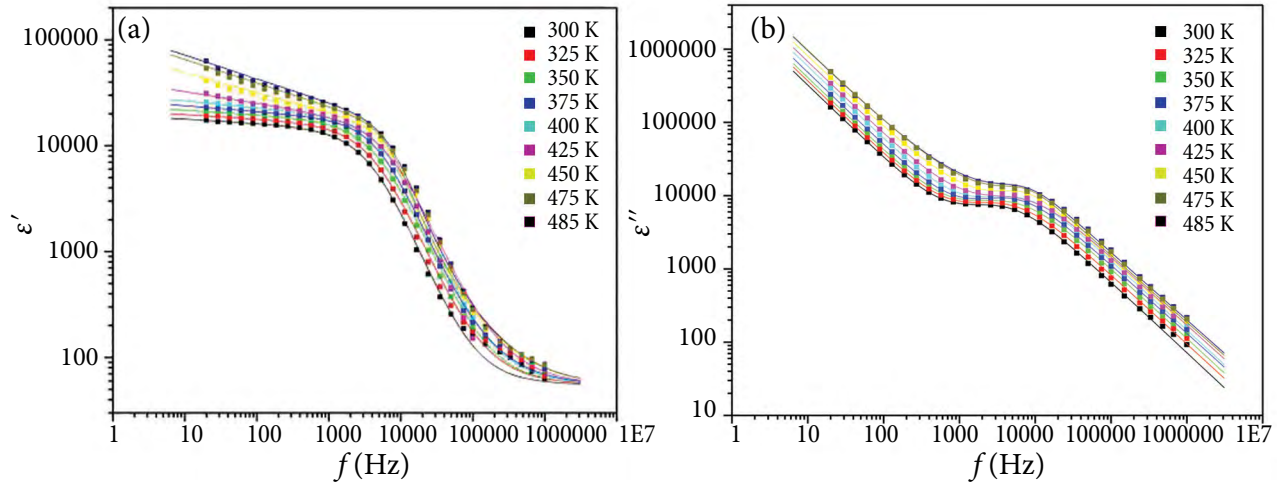

Fig. 2. Real (a) and imaginary (b) parts of the dielectric constant at different temperatures. The solid lines fit the data points with the Raicu relation.

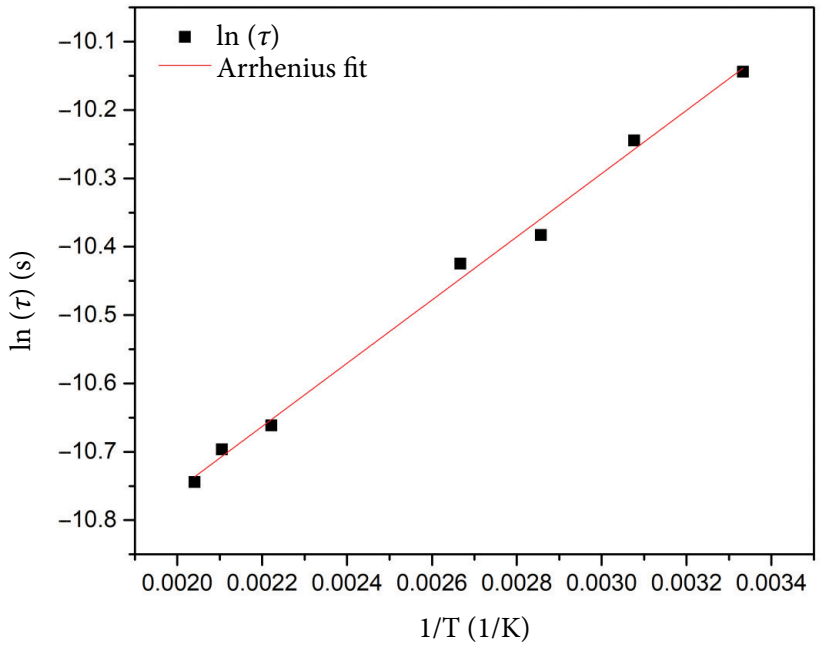

Fig. 3. Inverse temperature dependence of the mean relaxation time in PZT ceramics. The data points are fitted using Eq. (2).

Here τ_0 represents the relaxation time for $T \to \infty$, E denotes the activation energy, and k symbolizes the Boltzmann constant.

Based on this fit, activation energy is equal to 436 K (37.6 meV). When heating a ferroelectric sample, a weak measuring field with an electric field strength of less than 10 V mm^{-1} is applied to it. This causes domain walls to vibrate. For the studied PZT samples, the process that occurs in this case has an energy on the order of $U \sim 40$ meV. This energy is indicative of the initial oscillations of the domain walls within the local potential well [23].

The complex impedance data, which consists of the real part (Z') and the imaginary part (Z''),

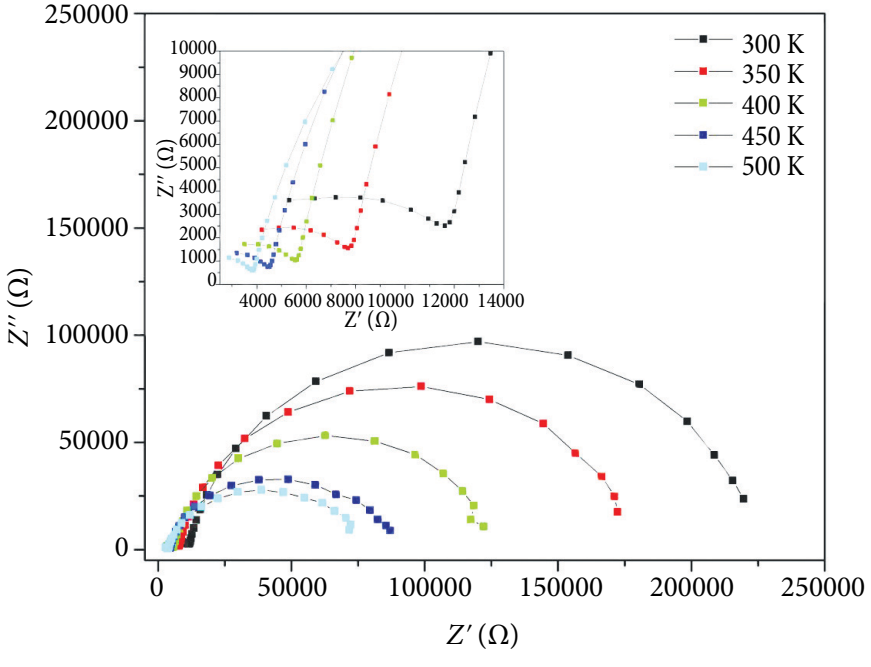

Fig. 4. Nyquist plot of Z' vs Z'' (with a characteristic resistivity of the high frequency region in the inset).

can also be represented as a Nyquist plot to display the characteristic impedance spectrum of the system, as shown in Fig. 4. Due to the significantly different time constants of individual *RC* elements, the individual semicircles of the PZT film and the LMSO film are clearly distinguishable in the temperature range. The real part of the characteristic impedance between the distinctive minima in the imaginary part (Z'') represents the macroscopic resistivity of LSMO (the left semicircle) and PZT (the right semicircle).

As the temperature increases, the diameter of the arc related to conduction in the bulk material decreases, and the centre of the semicircular arc moves closer to the origin of the complex plane plot. The movement of the origin of the semicircular arc toward the centre of the complex plane plot signifies a reduction in the sample's resistive characteristics. This change is linked to the increase in temperature and is attributed to grain boundary conduction. The primary source of dielectric response is evidently intrinsic for all the examined samples, as evident from the Nyquist plots.

4. Conclusions

High-quality epitaxial $PbZr_{0.2}Ti_{0.8}O_3$ films were successfully produced using the pulsed laser deposition (PLD) technique. Those films exhibited a remanent polarization of 93 $\mu C/cm^2$, attributed to the internal strains resulting from the lattice constant and the thermal expansion coefficient mismatch. Frequency dependence was accurately fitted with the Raicu relation and explains the low-frequency region of the plot that shows the change of the behaviour of our material from a dielectric-like behaviour to that of a semiconductor. The analysis of the Nyquist diagram revealed the presence of two distinct relaxation regions, which were associated with the resistivity of both the PZT and LSMO layers. This change is linked to the increase in temperature and is attributed to grain boundary conduction, and the primary source of dielectric response is evidently intrinsic for all the examined samples.

References

[1] O. Auciello, Science and technology of thin films and interfacial layers in ferroelectric and high-dielectric constant heterostructures and application to devices, J. Appl. Phys. **100**, 051614 (2006).

[2] J.F. Scott, Applications of modern ferroelectrics, Science **315**, 954–959 (2007).

[3] L.P. Silva Neto, J.O. Rossi, and A.R. Silva, Applications of PZT dielectric ceramics in high-energy storage systems, Mater. Sci. Forum **727–728**, 505–510 (2012).

[4] D.C. Lupascu, J. Nuffer, J.S. Wallace, and J. Rodel, Role of crack formation in the electric fatigue behavior of ferroelectric PZT ceramics, Proc. SPIE **3992**, 209–216 (2000).

[5] A.S. Sigov, K.A. Vorotilov, and O.M. Zhigalina, Effect of lead content on microstructure of sol-gel PZT structures, Ferroelectrics **433**, 146–157 (2012).

[6] L.M. Denis-Rotella, G. Esteves, J. Walker, H. Zhou, J.L. Jones, and S. Trolier-McKinstry, Residual stress and ferroelastic domain reorientation in declamped {001} $Pb(Zr_{0.3}Ti_{0.7})O_3$ films, IEEE Trans. Ultrason. Ferroelectr. Freq. Control **68**(2), 259–272 (2021).

[7] G.L. Brennecka, W. Huebner, B.A. Tuttle, and P.G. Clem, Use of stress to produce highly oriented tetragonal lead zirconate titanate (PZT 40/60) thin films and resulting electrical properties, J. Am. Ceram. Soc. **87**(8), 1459–1465 (2004).

[8] S. Gebhardt, L. Seffner, F. Schlenkrich, and A. Schonecker, PZT thick films for sensor and actuator applications, J. Eur. Ceram. Soc. **27**, 4177–4180 (2007).

[9] L. Song, S. Glinsek, and E. Defay, Toward low-temperature processing of lead zirconate titanate thin films: Advances, strategies, and applications, Appl. Phys. Rev. **8** (2021).

[10] M. Veith, M. Bender, T. Lehnert, M. Zimmer, and A. Jakob, Novel single-source precursors for the fabrication of $PbTiO_3$, $PbZrO_3$ and $Pb(Zr_{1-x}Ti_x)O_3$ thin-films by chemical vapor deposition, Dalton Trans. **40**, 1175–1182 (2011).

[11] Y. Yamasaki, Y. Yokota, H. Shima, and H. Uchida, One-axis-oriented growth of PZT thin films on transparent glass substrates using metal oxide nanosheets, Jpn. J. Appl. Phys. **61**, SN1006 (2022).

[12] G. Tan, S.H. Kweon, and I. Kanno, Piezoelectric properties of epitaxial Pb(Zr,Ti)O_3 thin films grown on Si substrates by the sol–gel method, Thin Solid Films **764**, 139612 (2023).

[13] R. Eason, S. Barrington, C. Grivas, T. May-Smith, and D. Shepherd, *Pulsed Laser Deposition of Thin Films: Applications-Led Growth of Functional Materials* (Wiley-Interscience John Wiley and Sons, 2006) pp. 383–420.

[14] I. Vrejoiu, D. Hesse, and M. Alexe, Single crystalline PZT films and the impact of extended structural defects on the ferroelectric properties, in: *Handbook of Advanced Dielectric, Piezoelectric and Ferroelectric Materials: Synthesis, Properties and Applications* (CRC Press, 2008) pp. 695–723.

[15] C. Huang, Z. Liao, M. Li, C. Guan, F. Jin, M. Ye, X. Zeng, T. Zhang, Z. Chen, Y. Qi, P. Gao, and L. Chen, A highly strained phase in $PbZr_{0.2}Ti_{0.8}O_3$ films with enhanced ferroelectric properties, Adv. Sci. **8**, 1–8 (2021).

[16] M. Španková, V. Štrbík, Š. Chromik, D.N. Zheng, J. Li, D. Machajdík, A. P. Kobzev, T. Plecenik, and M. Sojková, Characterization of epitaxial LSMO films grown on STO substrates, Acta Phys. Pol. A **131**, 848–850 (2017).

[17] Z.G. Ban, S.P. Alpay, F. He, B.O. Wells, and X.X. Xi, Multiple relaxation mechanisms in $SiTiO_3/SrRuO_3$ heterostructures, Appl. Phys. Lett. **84**, 4848–4850 (2004).

[18] I. Vrejoiu, G.L. Rhun, L. Pintilie, D. Hesse, M. Alexe, and U. Gosele, Intrinsic ferroelectric properties of strained tetragonal $PbZr_{0.2}Ti_{0.8}O_3$ obtained on layer-by-layer grown, defect-free single-crystalline films, Adv. Mater. **18**, 1657–1661 (2006).

[19] M.J. Haun, E. Furman, S.J. Jang, and L.E. Cross, Thermodynamic theory of the lead zirconate-titanate solid solution system, part V: Theoretical calculations, Ferroelectrics **99**, 63–86 (1989).

[20] J.D.S. Guerra, R.J. Portugal, A.C. Silva, R. Guo, and A.S. Bhalla, Investigation of the conduction processes in PZT-based multiferroics: Analysis from Jonscher's formalism, Phys. Status Solidi B **251**, 1020–1027 (2014).

[21] S. Dussan, A. Kumar, J.F. Scott, and R.S. Katiyar, Magnetic effects on dielectric and polarization behavior of multiferroic heterostructures, Appl. Phys. Lett. **96**, 072904 (2010).

[22] V. Raicu, Dielectric dispersion of biological matter: Model combining Debye-type and "universal" responses, Phys. Rev. E **60**, 4677–4680 (1999).

[23] D.V. Kuzenko, Temperature-activation mechanism of the temperature dependence of the dielectric constant of ferroelectric ceramics PZT, J. Adv. Dielectr. **12**, 1–7 (2022).

PUSIAU LAIDŪS PLONIEJI ŠVINO CIRKONATO TITANATO SLUOKSNIAI, IŠAUGINTI IMPULSINIU LAZERINIU GARINIMU

V. Haronin [a], M. Alexe [b], R. Grigalaitis [a], J. Banys [a]

[a] *Vilniaus universiteto Fizikos fakultetas, Vilnius, Lietuva*

[b] *Voriko universiteto Fizikos katedra, Koventris, JK*

Santrauka

Nevienalyčiai dariniai, kuriuos sudaro $PbZr_{0,2}Ti_{0,8}O_3$ epitaksiniai sluoksniai ant $SrTiO_3$ (100) padėklo su $La_{0,67}Sr_{0,33}MnO_3$ apatiniu elektrodu, buvo išauginti impulsinio lazerinio nusodinimo būdu. Suformuoti plokščiojo kondensatoriaus dariniai buvo tiriami dielektrine spektroskopija ir pjezoelektriniais matavimais. Pjezoelektrinės kilpos poslinkis rodo, kad bandinyje stebimas nedidelis vidinis liktinis laukas, nukreiptas į viršutinį (vario) elektrodą. Buvo atlikti temperatūriniai matavimai 300–500 K diapazone, siekiant gauti informacijos apie dažninį metalo-feroelektriko-metalo (MFM) darinio atsaką ir išanalizuoti elektronų injekcijos per du Šotkio tipo kontaktus poveikį. Pastebėta, kad krūvio injekcija labai padidina žemadažnį šių nevienalyčių darinių laidumą.